Pax7 is required for establishment of the xanthophore lineage in zebrafish embryos

Hanna Nord[a], Nils Dennhag[a], Joscha Muck[a,b], and Jonas von Hofsten[a,c,*]
[a]Umeå Centre for Molecular Medicine and [c]Department for Integrative Medical Biology, Umeå University, 90187 Umeå, Sweden; [b]Max Planck Institute for Biology of Ageing, 50931 Cologne, Germany

ABSTRACT **The pigment pattern of many animal species is a result of the arrangement of different types of pigment-producing chromatophores. The zebrafish has three different types of chromatophores: black melanophores, yellow xanthophores, and shimmering iridophores arranged in a characteristic pattern of golden and blue horizontal stripes. In the zebrafish embryo, chromatophores derive from the neural crest cells. Using *pax7a* and *pax7b* zebrafish mutants, we identified a previously unknown requirement for Pax7 in xanthophore lineage formation. The absence of Pax7 results in a severe reduction of xanthophore precursor cells and a complete depletion of differentiated xanthophores in embryos as well as in adult zebrafish. In contrast, the melanophore lineage is increased in *pax7a/pax7b* double-mutant embryos and larvae, whereas juvenile and adult *pax7a/pax7b* double-mutant zebrafish display a severe decrease in melanophores and a pigment pattern disorganization indicative of a xanthophore- deficient phenotype. In summary, we propose a novel role for Pax7 in the early specification of chromatophore precursor cells.**

Monitoring Editor
Marianne Bronner
California Institute of Technology

Received: Dec 7, 2015
Revised: Mar 29, 2016
Accepted: Apr 1, 2016

INTRODUCTION

Most animals have evolved characteristic color patterns serving as protection from harmful radiation, species recognition, and intraspecies communication and sexual attraction. The pigment pattern in zebrafish (*Danio rerio*) is a result of the arrangement of different types of pigment cells, or chromatophores, originating from the neural crest cells (Dushane, 1934; Kelsh *et al.*, 1996). Zebrafish have three different types of chromatophores: black melanophores, yellow xanthophores, and shimmering iridophores. The chromatophores are arranged in two distinct age-dependent patterns—the embryo/early larvae pattern and the adult pattern—separated by a metamorphic interphase (Kimmel *et al.*, 1995; Parichy and Spiewak, 2015). The chromatophores in the embryo/early larvae are directly derived from neural crest cells (Kelsh *et al.*, 1996; Parichy, 2006), whereas adult melanophores and iridophores originate from specific progenitor cell populations that both reside at the dorsal root ganglia (DRG; Budi *et al.*, 2011; Dooley *et al.*, 2013; Singh *et al.*, 2014). Adult xanthophores are derived from larval xanthophores that proliferate during the metamorphic period (Mahalwar *et al.*, 2014); however, adult xanthophores formed independently of larval xanthophores have also been identified (McMenamin *et al.*, 2014).

The neural crest is a group of multipotent precursor cells that give rise to several different cell types in the vertebrate embryo, such as neurons and glia cells, craniofacial cartilage, and pigment cells (Le Douarin *et al.*, 2004; Mayor and Theveneau, 2013; Simoes-Costa and Bronner, 2015). The paired box homeodomain transcription factors Pax3 and Pax7 are closely related and have important roles during neural crest development (Monsoro-Burq, 2015). Pax3 mutant mice have severely reduced neural crest and thus show defects in all neural crest derivatives (Auerbach, 1954; Epstein *et al.*, 1993; Tremblay and Gruss, 1994). In contrast, although Pax7 is expressed in neural crest cells in mouse (Jostes *et al.*, 1990; Mansouri *et al.*, 1996; Lang *et al.*, 2003; Murdoch *et al.*, 2012), no obvious neural crest phenotype is observed in Pax7 mutant mice except for facial malformations, indicating a cephalic neural crest defect (Mansouri *et al.*, 1996). In chick, Pax7 is required for neural crest specification during gastrulation (Basch *et al.*, 2006), and in medaka embryos, *pax7a* has been implied to be essential for the development of a shared xanthophore/leucophore progenitor cell derived

This article was published online ahead of print in MBoC in Press (http://www.molbiolcell.org/cgi/doi/10.1091/mbc.E15-12-0821) on April 6, 2016.

*Address correspondence to: Jonas von Hofsten (jonas.von.hofsten@umu.se).

Abbreviations used: dpf, days postfertilization; DRG, dorsal root ganglia; hpf, hours postfertilization; TALEN, transcription activator–like effector nuclease; wt, wild type.

Supplemental Material can be found at:
http://www.molbiolcell.org/content/suppl/2016/04/03/mbc.E15-12-0821v1.DC1.html

from the neural crest (Kimura *et al.*, 2014; Nagao *et al.*, 2014). Furthermore, Pax7 is expressed by myoblasts in amniotes (Lacosta *et al.*, 2005). Morpholino-based antisense RNA knockdown studies in zebrafish suggest that Pax3 is required for the specification of enteric neurons and xanthoblasts and that in the absence of Pax3, the number of xanthophores is decreased in correlation with an increase in melanophore cell number (Minchin and Hughes, 2008). Expression of Pax7 has been reported in cells of the xanthophore lineage, and knockdown experiments suggest that Pax7a is involved in the xanthophore pigmentation process but dispensable for the formation of the xanthophore lineage (Minchin and Hughes, 2008). The precise role of Pax7 in the specification of neural crest–derived lineages in zebrafish remains unclear.

The zebrafish genome contains two *pax7* genes—*pax7a* and *pax7b*. In this study, we introduce two new zebrafish lines mutant for *pax7a* and *pax7b*. We present evidence for a previously unknown role for Pax7 in the establishment of the xanthophore lineage in which xanthophores are lost and the embryonic/larval melanophore lineage is expanded in the absence of Pax7. Moreover, in addition to a continuous absence of xanthophores, juvenile and adult *pax7a/pax7b* double-mutant zebrafish display a melanophore phenotype with a significant decrease in the number of melanophores and a defective pigment-patterning process. In summary, we present a new role for Pax7 in the zebrafish pigmentation process.

RESULTS

Generation of *pax7a* and *pax7b* mutant zebrafish

Using transcription activator-like effector nucleases (TALENs) targeting exon 1 of the *pax7a* and *pax7b* loci, respectively, we generated mutant zebrafish lines exhibiting premature stop codons and dysfunctional proteins (Figure 1, A and B). The TALENs introduce double-strand DNA breaks that, when repaired, result in random nucleotide deletions and insertions. Initially, five different *pax7a* and six different *pax7b* mutation variants were identified in the F_1 generation, and strains carrying frameshift-causing deletions, one for each gene, were used to establish stable mutant lines (Figure 1, A and B). Immunofluorescence staining using an antibody detecting Pax7 (Kawakami *et al.*, 1997) on F_2 zebrafish embryos 24 h postfertilization (hpf) confirmed the lack of Pax7 epitopes in *pax7a/pax7b* double-mutant embryos (Figure 1C).

The melanophore lineage is expanded in *pax7* mutant embryos and larvae

The embryonic/early larval zebrafish has distinct stripes of melanophores spanning in an anterior-to-posterior manner along the most dorsal, medial, and ventral parts of the body and covering the ventral part of the yolk sac. The iridophores can be found sparsely intermingled with the melanophores, whereas xanthophores are widely scattered along the head and the most dorsal part of the fish, resulting in a yellow tone (Kimmel *et al.*, 1995; Kelsh *et al.*, 1996; Quigley and Parichy, 2002; Parichy and Turner, 2003b). The first visually detectable pigment cells in zebrafish embryos are black melanophores (Kimmel *et al.*, 1995). At 3 d postfertilization (dpf), *pax7a* and *pax7b* single-mutant embryos have normal numbers, whereas *pax7a/pax7b* double-mutant embryos have significantly more melanophores on the crown of the head than do wild-type (wt) siblings (Figure 2A). A similar melanophore phenotype is found in zebrafish *pax7a/pax7b* double-mutant larvae at 6 dpf, in which the number of melanophores is significantly higher than in wt siblings on both the crown of the head and in the dorsal larval melanophore stripe (Figure 2, B–E). Moreover, the melanophores of *pax7a/pax7b* double-mutant larvae appear smaller (Figure 2, D and E). No consistent iridophore phenotype is observed in any of the *pax7* mutant larvae (Figure 2, D and E).

To elucidate the role of Pax7 in melanophore formation, we analyzed the expression patterns of several chromatophore markers in wt and *pax7a/pax7b* double-mutant embryos at 24 hpf. No obvious effect in expression of the neural crest marker *sox10* was detected except for a somewhat disorganized expression pattern mainly in the midbrain–hindbrain region of the *pax7a/pax7b* double-mutant embryos (Figure 3A). *mitfa* (microphthalmia-associated transcription factor a) is predominantly expressed in melanoblasts and possibly in xanthoblasts (Lister *et al.*, 1999; Minchin and Hughes, 2008), and *dct* (dopachrome tautomerase) is a melanophore-specific gene (Kelsh *et al.*, 2000). A significant increase in *mitfa*$^+$ and *dct*$^+$ cells is observed in *pax7a/pax7b* double-mutant embryos compared with wt siblings at 24 hpf (Figure 3, B–D), which agrees with the increase in melanized melanophores detected in *pax7a/pax7b* double mutants at older stages (Figure 2).

Pax7 is required for proper xanthophore formation

To analyze xanthophore development in the absence of functional Pax7, we analyzed the expression patterns of several xanthophore lineage markers in *pax7a/pax7b* double-mutant embryos at 24 hpf (Figure 4). The expression of *gch2* is dramatically reduced in *pax7a/pax7b* double-mutant embryos compared with wt siblings (Figure 4A). *gch2* encodes GTP cyclohydrolase 2 and is specifically expressed in xanthoblasts and to some extent in melanoblasts (Parichy *et al.*, 2000; Pelletier *et al.*, 2001; Minchin and Hughes, 2008). The zebrafish colony-stimulating factor 1 receptor (*csf1r*) is expressed by premigratory and migratory xanthophore precursors and is required for embryonic xanthophore precursor morphogenesis (Parichy *et al.*, 2000). Compared to wt siblings, *pax7a/pax7b* double-mutant embryos have a severe reduction of *csf1r*$^+$ neural crest cells; only a few, weakly stained *csf1r*$^+$ cells can be detected in the head region and in the premigratory neural crest region along the most dorsal part of the trunk (Figure 4B). A similar expression pattern is detected for the xanthophore differentiation marker xanthine dehydrogenase (*xdh*) in *pax7a/pax7b* double mutants (Figure 4C). In agreement with previous studies (Parichy *et al.*, 2000), double in situ hybridization shows that several chromatoblasts in wt embryos coexpress *xdh* and *mitfa* (Supplemental Figure S1), implying a certain amount of chromatoblast plasticity at this stage, which is also true for *pax7a/pax7b* double-mutant embryos (Supplemental Figure S1).

To visualize differentiated xanthophores at early stages, before any yellow color is obvious, UV light can be used to induce pteridine autofluorescence (Kelsh *et al.*, 1996; Le Guyader and Jesuthasan, 2002). Subjecting wt embryos at 48 hpf to UV light (340–380 nm) results in strongly fluorescing xanthophores in the trunk (Figure 4D); however, no similar autofluorescing cells are detected when *pax7a/pax7b* double-mutant embryos are treated similarly (Figure 4D). Taken together, in the absence of functional Pax7, the pool of chromatophore precursor cells expressing xanthophore lineage markers is severely reduced, and there is an absence of differentiated xanthophores.

pax7a overexpression can rescue the xanthophore phenotype

To detect more mature xanthophores, we reared embryos in methylene blue, which has been reported to specifically label the pterinosome pigment organelles found in terminally differentiated xanthophores (Le Guyader and Jesuthasan, 2002). At 5 dpf, the wt embryos display a yellow tone along the most dorsal part of the body, as well as methylene blue–colored, stellate-shaped xanthophores along the

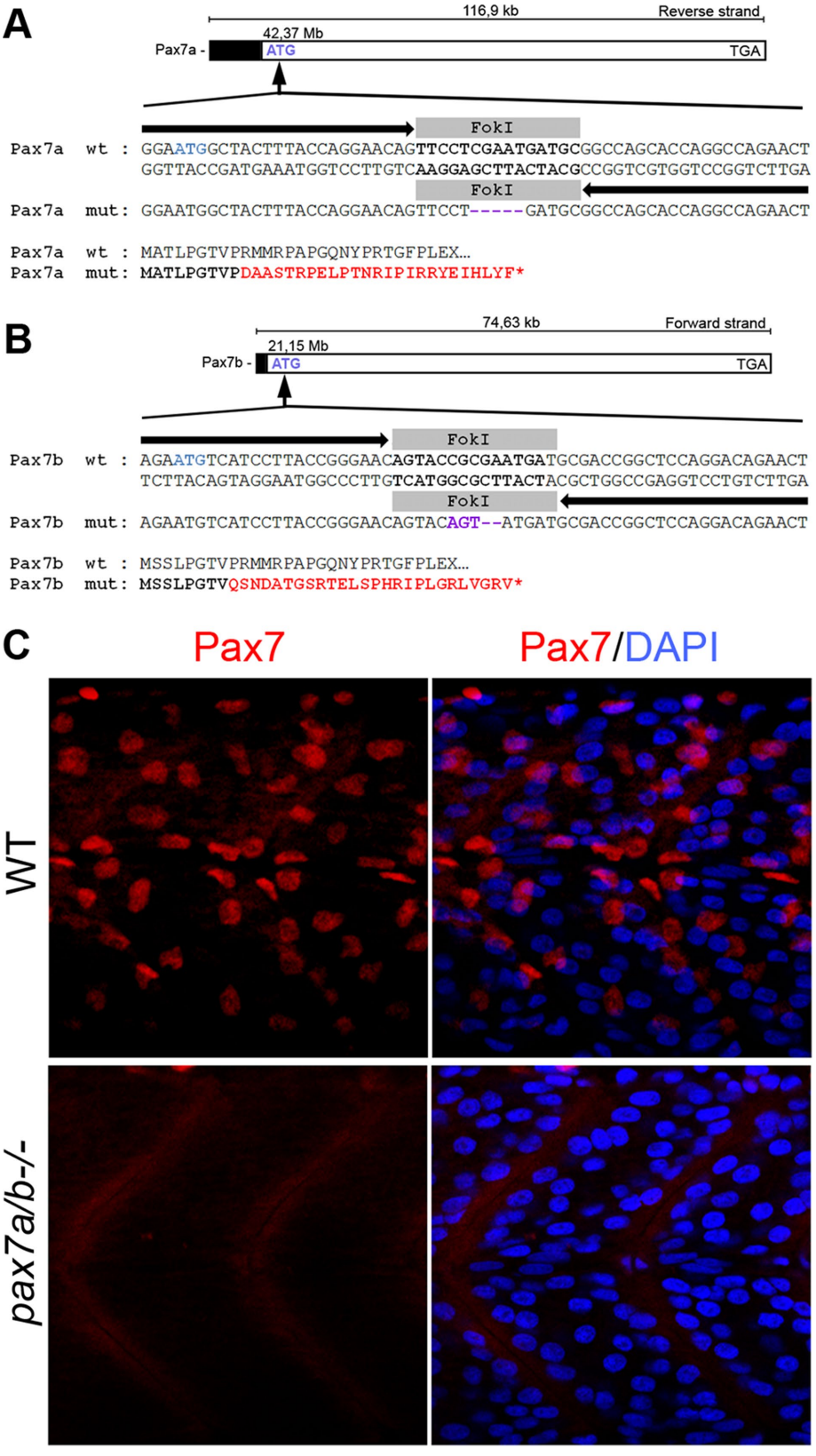

FIGURE 1: Generation of *pax7a* and *pax7b* mutants using TALENs. Schematic overview of TALEN-induced deletions resulting in frameshift mutations in genes (A) *pax7a* and (B) *pax7b* on chromosome 11. Black arrows represent the left and right TALEN sequences, and the gray box represents the spacer sequence indicating the *Fok*I cut site. Purple indicates the insertion of mismatched nucleotides, and red indicates mismatched amino acids. (C) Lateral view of 24-hpf wt embryo and *pax7a/pax7b* double-mutant trunk immunofluorescently analyzed using a Pax7 antibody (red). DAPI is used to visualize nuclei.

midline and on the head (Figure 5A). However, in agreement with previous results, no yellow tone was detected, and no methylene blue–stained xanthophores were ever observed in the *pax7a/pax7b* double-mutant embryos (Figure 5B).

To rescue *pax7* expression in the chromatophore precursor population at the time point of chromatophore specification, we injected a construct in which 4118 base pairs upstream of the translational start of *sox10* drives the expression of *pax7a* specifically in the neural crest cells into *pax7a/pax7b* double-mutant embryos. Previous studies showed that a region 1252 base pairs upstream of the *sox10* transcriptional start (3731 base pairs upstream of the translational start) contains all regulatory elements sufficient to drive a mosaic GFP expression resembling the expression pattern and timing of the *sox10* gene (Dutton *et al.*, 2008). At 5 dpf, several methylene blue–stained xanthophores can be identified in the *pax7a/pax7b* double mutants injected with *sox10*:*pax7a* (Figure 5C), and sporadic xanthophores can be detected in the same fish at adult stages (Supplemental Figure S2), suggesting that Pax7 is capable of rescuing the xanthophore population. To test whether Pax7 alone is sufficient to switch all chromatophore precursor cells into cells of the xanthophore lineage, we injected *pax7a* mRNA into wt embryos. General *pax7a* overexpression often results in defective eye formation and other somatic malformations; however, no decrease in melanophore cell number (Supplemental Figure S3A) or overrepresentation of xanthophores was detected at 6 dpf (Supplemental Figure S3B).

Other neural crest–derived cell lineages form normally in *pax7a/pax7b* double mutants

Neural crest cells are multipotent stem cells that differentiate into several different cell types. In addition to pigment cells, the neural crest gives rise to craniofacial cartilage and bone structures, most of the cephalic peripheral nervous system, DRG, and surrounding satellite glia, as well as the enteric neurons of the digestive tract (Mayor and Theveneau, 2013). At 3 dpf, no chondrocyte phenotype is observed in the developing cranial structures of *pax7a/pax7b* double-mutant embryos, as indicated by Alcian blue staining (Supplemental Figure S4A). Furthermore, normal formation of the craniofacial skeleton in *pax7a/pax7b* double-mutant zebrafish was confirmed using calcein to stain calcified bone (Supplemental Figure S4, B and C). To analyze whether the enteric nervous system forms normally in

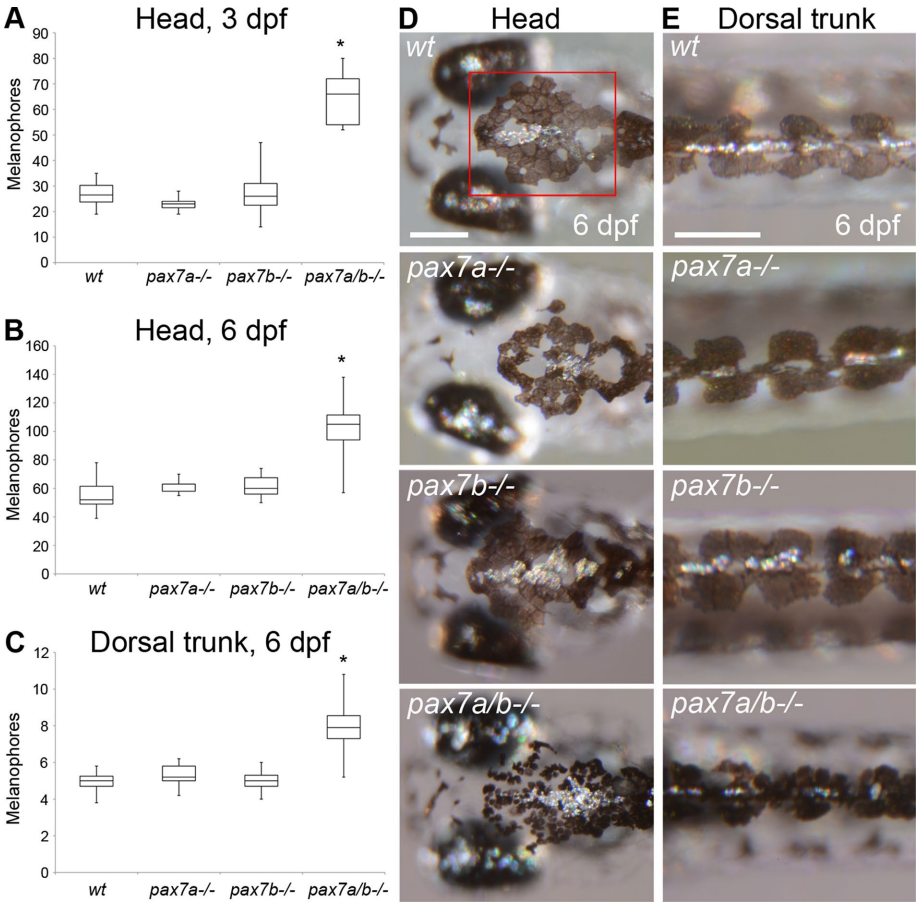

FIGURE 2: The *pax7a/pax7b* double-mutant embryo and larvae display an increased number of melanophores. (A) Number of melanophores on the crown of the head between the midbrain–hindbrain border and the most anterior part of the dorsal larval melanophore stripe in wt ($n = 16$), *pax7a*$^{-/-}$ ($n = 11$), *pax7b*$^{-/-}$ ($n = 15$), and *pax7a/pax7b* double-mutant ($n = 11$) zebrafish embryos at 3 dpf. The *pax7a/pax7b* double mutants differ from all other groups with $p < 0.001$. (B) Number of melanophores on the crown of the head between the midbrain–hindbrain border and the most anterior part of the dorsal larval melanophore stripe in wt ($n = 11$), *pax7a*$^{-/-}$ ($n = 5$), *pax7b*$^{-/-}$ ($n = 7$), and *pax7a/pax7b* double-mutant ($n = 11$) zebrafish larvae at 6 dpf. The *pax7a/pax7b* double mutants differ from all other groups with $p < 0.001$. The red box in D indicates area of counting. (C) Number of melanophores/somite in the dorsal larval melanophore stripe of wt ($n = 12$), *pax7a*$^{-/-}$ ($n = 5$), *pax7b*$^{-/-}$ ($n = 11$), and *pax7a/pax7b* double-mutant ($n = 10$) zebrafish larvae at 6 dpf. Somites 8–12 were counted. The *pax7a/pax7b* double mutants differ from all other groups with $p < 0.001$. (D) Head melanophore phenotype in wt, *pax7a*$^{-/-}$, *pax7b*$^{-/-}$, and *pax7a/pax7b* double-mutant zebrafish larvae at 6 dpf. (E) Dorsal larval melanophore stripe phenotype in wt, *pax7a*$^{-/-}$, *pax7b*$^{-/-}$, and *pax7a/pax7b* double-mutant zebrafish larvae at 6 dpf. Comparisons between groups by one-way ANOVA or Kruskal–Wallis ANOVA on ranks with Student's–Newman–Keuls or Dunn's post hoc contrast test for parametric and nonparametric data. Scale bar, 200 µm.

the absence of Pax7, we analyzed HuC/D expression in embryos 4 dpf; the formation of enteric neurons in the gut of *pax7a/pax7b* double-mutant embryos seemed unaffected (Supplemental Figure S5). In addition, HuC/D-positive DRG appear to form normally in *pax7a/pax7b* double-mutant embryos (Supplemental Figure S5). Thus involvement of Pax7 was only observed in the neural crest cell population, which differentiates into chromatophores.

The expanded melanophore lineage is not maintained in juvenile and adult *pax7a/pax7b* double mutants

At juvenile stages, the zebrafish enters a metamorphic phase in which the embryonic/larvae pigment pattern is transformed into an adult pigment pattern with characteristic thick, dark stripes separated by lighter interstripes spanning the anterior–posterior axis of the fish (Parichy and Turner, 2003b; Parichy, 2006; Hirata *et al.*, 2005). To assess whether Pax7 plays a role in the metamorphic pigment-patterning process, we analyzed the pigment of juvenile zebrafish at 30 dpf. We counted the number of melanophores on the flank just above the pectoral fins. Compared to wt siblings, a significant decrease of melanophores can be detected in the *pax7a/pax7b* double-mutant fish, whereas *pax7a* and *pax7b* single mutants do not show any significant difference in melanophore number (Figure 6). To investigate how the melanophores behave during the metamorphic period in the absence of Pax7, we repeatedly observed the pigment pattern of juvenile zebrafish from 25 to 46 dpf (Supplemental Figure S6). Monitoring single melanophores over time showed that almost all melanophores identified at 25 dpf are still present at 46 dpf in wt zebrafish. During this period, new melanophores appear, which become organized into dark, melanophore-rich stripes separated by xanthophore-rich interstripes (Supplemental Figure S6A). In *pax7a/pax7b* double mutants, the majority of melanophores observed at 25 dpf subsequently disappear, and although new melanophores appear over time, their presence does not compensate for the severe loss observed at 46 dpf (Supplemental Figure S6B). The majority of the melanophores in the *pax7a/pax7b* double mutants are at first organized much like the wt into dorsal, medial, and ventral stripes, as well as covering the yolk sac; however, with time, this organization is disrupted, the melanophores in the *pax7a/pax7b* double mutants fail to organize into a striped pattern, and new melanophores appear in a scattered pattern (Supplemental Figure S6B).

Melanophores and a low number of iridophores and stellate-shaped xanthophores predominantly make up the dark stripes in adult zebrafish, whereas interstripes consist of large numbers of iridophores and round xanthophores (Figure 7A; Mahalwar *et al.*, 2014; Eom *et al.*, 2015; Singh and Nusslein-Volhard, 2015). In comparison to wt zebrafish (Figure 7A), the pigment pattern of *pax7a* and *pax7b* single-mutant zebrafish appears to be unaffected (Figure 7, B and C). However, similar to juvenile stages, adult *pax7a/pax7b* mutant zebrafish display a severe depletion of melanophores (Figure 7D). In addition, a defect in the arrangement of the residual melanophores is observed in *pax7a/pax7b* mutant zebrafish, in which melanophores are found scattered all over the flank, although a general tendency of stripe formation can be distinguished (Figure 7D). Furthermore, in agreement with embryonic/larval stages, no xanthophores are detected in juvenile and adult *pax7a/pax7b* double-mutant zebrafish (Figures 6A and 7D). The iridophores in juvenile and adult zebrafish appear unaffected by the absence of Pax7 (Figures 6A and 7).

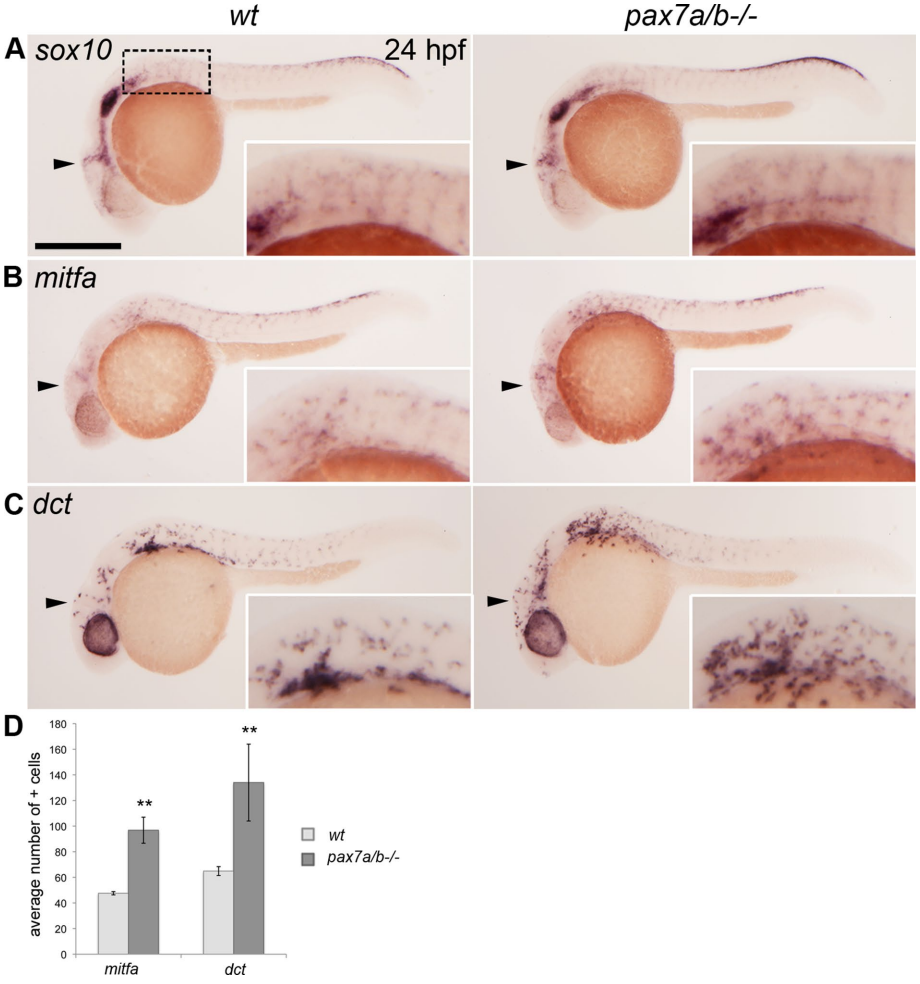

FIGURE 3: The *pax7a/pax7b* double mutants have an increased number of melanoblasts. Whole-mount in situ hybridization on wt siblings and *pax7a/pax7b* double-mutant zebrafish embryo at 24 hpf showing the expression of (A) *sox10* ($n > 50$ for siblings and $n = 7$ for *pax7a/pax7b* double mutants), (B) *mitfa* ($n = 5$ and 5), and (C) *dct* ($n = 7$ and 3). (D) Average number of *mitfa*$^+$ and *dct*$^+$ cells in the region anterior to the first somite on one side of wt siblings and *pax7a/pax7b* double-mutant embryos at 24 hpf; positive cells in the eye were excluded. Student's *t* test was used to calculate significance; $^{**}p < 0.01$. Error bars indicate SEM. Box indicates area of enlargement visualized in insets. Arrowheads indicate head region where changes in expression can be detected. Scale bar, 200 μm.

DISCUSSION

In this study, we assess the involvement of Pax7 in zebrafish pigment formation from embryonic to adult stages. By generating *pax7a* and *pax7b* mutant zebrafish lines, we demonstrate an early role for Pax7 in the development of neural crest–derived chromatophore precursor cells. In the absence of Pax7, there is a severe depletion of xanthophore precursor cells, a complete lack of differentiated xanthophores, and an expansion of the embryonic/larval melanophore lineage. In contrast, adult Pax7 mutants have a dramatic reduction of melanophores and disrupted pigment pattern.

Expression of Pax7 was shown in the zebrafish neural crest cells specifically in the xanthophore lineage (Minchin and Hughes, 2008). Knocking down *pax7a* using morpholinos suggests that Pax7a is dispensable for xanthoblast fate specification and required for the xanthophore pigmentation process, in which *pax7a* morphants have a reduction of yellow pigment but a normal number of methylene blue–colored xanthophores (Minchin and Hughes, 2008). However, in *pax7a/pax7b* double-mutant zebrafish embryos, we observe a severe reduction in expression of the xanthophore lineage markers *gch2*, *xdh*, and *csf1r* and a complete lack of methylene blue–colored and autofluorescing xanthophores (Figures 4 and 5), suggesting a deficiency of differentiated xanthophores. Thus, in the absence of Pax7, chromatophore precursor cells expressing xanthophore lineage markers are still present but severely reduced in number. There is, however, no formation of a xanthophore population. This suggests that Pax7 is involved in establishing a proper population of xanthoblasts and xanthophores; whether this is via xanthophore differentiation, xanthoblast survival, or chromatophore fate decision remains to be determined.

In contrast to the decrease in xanthophore precursors, a significant increase in cells expressing the melanophore lineage markers *mitfa* and *dct*, as well as in melanized melanophores, is observed in zebrafish embryos and larvae (Figures 2 and 3). This could imply that Pax7 is involved in instructing chromatophore precursor cells into adopting a xanthophore cell fate and that, in the absence of functional Pax7, these precursors take on a melanophore fate. However, the possibility cannot be excluded that the melanophore phenotype observed in *pax7a/pax7b* double-mutant embryos and larvae is a nonautonomous effect caused or enhanced by the absence of Pax7 and the xanthophore deficiency. There are studies indicating that Pax7 is expressed in some melanophores of the dorsal stripe at 48 hpf (Lacosta *et al.*, 2007), which could imply that Pax7 might act directly on the melanophore lineage.

We find that a proportion of the chromatophores coexpress *xdh* and *mitfa* (Supplemental Figure S1), suggesting a certain plasticity of this population, agreeing with previous studies indicating the presence of pluripotent chromatophore precursor cells (Bagnara *et al.*, 1979; Parichy *et al.*, 2000; Parichy and Turner, 2003a; Pelletier *et al.*, 2001; Minchin and Hughes, 2008; Curran *et al.*, 2010). A model has been proposed in which melanophores and iridophores share a common *mitfa*$^+$ precursor cell in zebrafish (Curran *et al.*, 2010). Furthermore, morpholino-based knockdown data suggest that Pax3 drives a xanthophore/melanophore fate switch in chromatophore precursor cells by which there is a loss of xanthophores and an increase in melanophores in the absence of Pax3 (Minchin and Hughes, 2008). In addition, several studies show coexpression of melanoblast and xanthoblasts markers (Parichy *et al.*, 2000; Parichy and Turner, 2003a; Pelletier *et al.*, 2001; Minchin and Hughes, 2008), and a common melanophore/xanthophore lineage has been observed in the fin of the zebrafish (Tu and Johnson, 2010, 2011). In medaka embryos, leucophores and xanthophores have similar specification and differentiation processes (Kimura *et al.*, 2014). In contrast, with the exception of the earliest-migrating neural crest cells, most zebrafish neural crest cells are proposed to be lineage restricted, producing

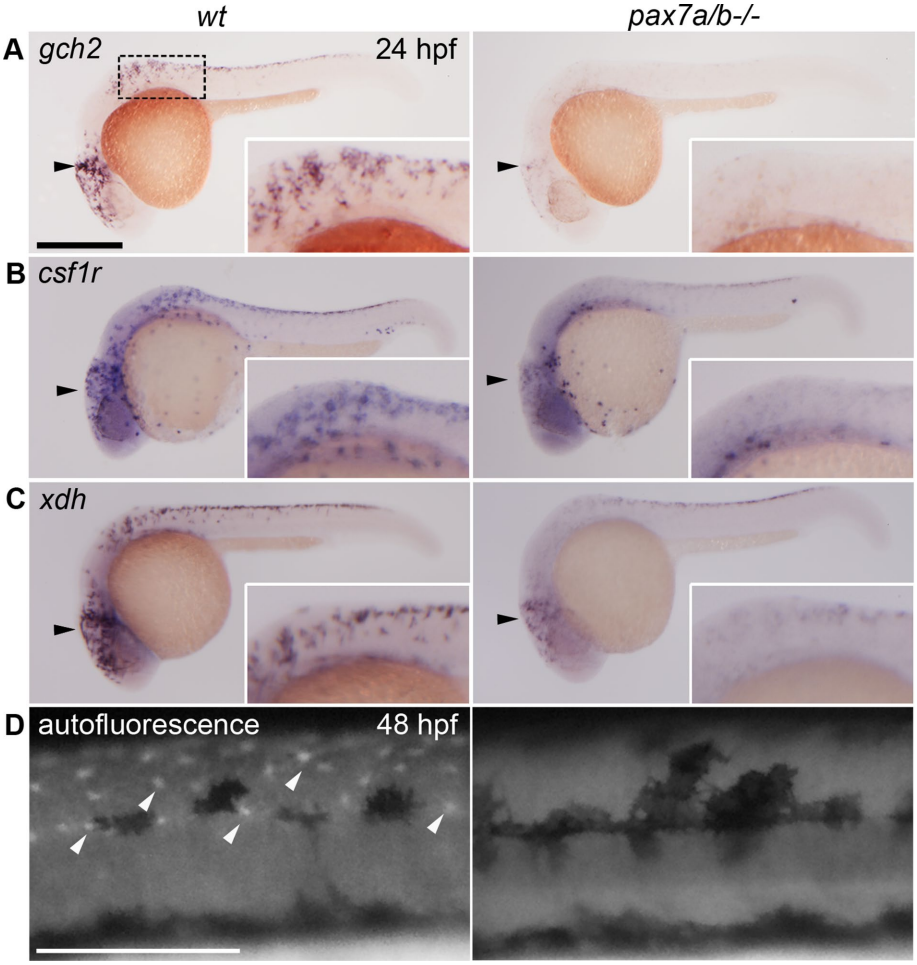

FIGURE 4: The *pax7a/pax7b* double-mutant embryos have a reduced xanthoblast pool and completely lack differentiated xanthophores. Whole-mount in situ hybridization on wt siblings and *pax7a/pax7b* double-mutant zebrafish embryo at 24 hpf showing the expression of (A) *gch2* ($n = 13$ for siblings and $n = 7$ for *pax7a/pax7b* double mutants), (B) *csf1r* ($n = 5$ and 3), and (C) *xdh* ($n = 3$ and 5). (D) Pteridine autofluorescence in wt and *pax7a/pax7b* double-mutant zebrafish embryo at 48 hpf. Box indicates area of enlargement visualized in insets. Black arrowheads indicate head region where changes in expression can be detected; white arrowheads indicate a subset of autofluorescing xanthophores. Scale bar, 200 µm.

single derivatives, and lineage analysis of neural crest progeny indicate that melanophores and unmelanized chromatophores might not derive from the same progenitors (Raible and Eisen, 1994).

Injecting *pax7a* mRNA into one-cell-stage embryos did not induce a significant melanophore-to-xanthophore fate switch (Supplemental Figure S3), implying that overexpression of *pax7a* alone is not sufficient to switch xanthophore/melanophore precursor cells into a xanthophore fate. However, it should be noted that injecting pure RNA is a very crude method, which could cause other interfering effects. Using a more sophisticated approach and injecting a construct in which the *sox10* promoter drives the expression of *pax7a*, we were able to overexpress *pax7a* specifically in neural crest cells during the time point for melanophore/xanthophore specification. This resulted in a rescue of xanthophores in *pax7a/pax7b* double-mutant larvae, which persisted in adult (Figure 5 and Supplemental Figure S2). This suggests that in *pax7a/pax7b* double-mutant embryos, there are still neural crest–derived precursor cells present with the ability to respond to *pax7a* and promote a xanthophore cell fate. This also indicates that the adult xanthophores at least in part derive from or are dependent on the embryonic xanthophore lineage. However, because the *pax7a* rescue is mosaic and a low number of xanthophores were formed, we were not able to assay how the melanophore cell number was affected in this experiment.

Pax7 mutant mice display facial malformations in the nose and the maxilla (Mansouri *et al.*, 1996). We analyzed the craniofacial cartilage and skeleton in several *pax7a/pax7b* double-mutant embryos and larvae, and although we observed individual variations in both mutant and wt zebrafish, we could not confirm any consistent defects caused by the absence of functional Pax7 (Supplemental Figure S4). In addition, we found no obvious effect on the development of neural crest–derived enteric neurons and DRG in *pax7/pax7b* double-mutant embryos (Supplemental Figure S5). Our study show a specific role for Pax7 in the neural crest–derived pigment lineage; however, we do not exclude a possible function for Pax7 in the development and specification process of other neural crest derivatives.

In contrast to the increase in melanophore cell number detected in *pax7a/pax7b* double-mutant zebrafish embryos and early larvae, *pax7a/pax7b* double-mutant juvenile and adult zebrafish display a severe reduction in melanophores and a disrupted melanophore organization compared with wt (Figures 6 and 7 and Supplemental Figure S6). We analyzed the pigment pattern of *pax7a/pax7b* mutant zebrafish during the larval-to-adult metamorphic period and found that when the analysis was initiated (25 dpf), the melanophore arrangement in pax7/pax7 mutants did not differ drastically from wt (Supplemental Figure S6). However, with time, the majority of the original melanophores in the *pax7a/pax7b* double mutant disappeared and possibly died, and although new melanophores appeared, there was still a dramatic reduction compared with wt zebrafish, and no stripe organization was observed (Supplemental Figure S6). This indicates that Pax7 either has a direct effect on the adult melanophore lineage or the melanophore shortage observed is a nonautonomous effect, possibly caused by the xanthophore deficit. In *csf1r* mutant zebrafish, xanthophores fail to develop, and the number of melanophores is reduced. Furthermore, the melanophore pattern is disrupted during the metamorphic period, similar to the *pax7a/pax7b* double mutant (Odenthal *et al.*, 1996; Parichy *et al.*, 2000; Parichy and Turner, 2003a; Maderspacher and Nusslein-Volhard, 2003; Frohnhofer *et al.*, 2013). In addition, xanthophores are important for melanophore survival (Parichy *et al.*, 2000; Parichy and Turner, 2003a), and proper communication between all three chromatophore types is necessary for normal pigment pattern formation (Maderspacher and Nusslein-Volhard, 2003; Frohnhofer *et al.*, 2013; Irion *et al.*, 2014; Eom *et al.*, 2015). Hence the melanophore phenotype that we detect in juvenile and adult *pax7a/pax7b* double-mutant zebrafish is likely caused by the absence of xanthophores and further indicates that there is a

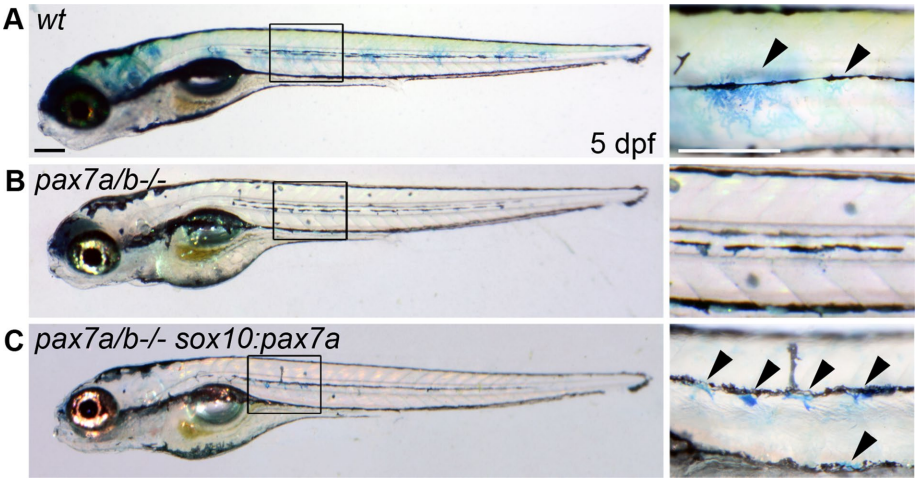

FIGURE 5: Xanthophores can be rescued by specifically expressing *pax7a* in the neural crest cells of *pax7a/pax7b* double mutants. (A) Wt sibling, (B) *pax7a/pax7b* double mutant, and (C) *pax7a/pax7b* double mutant injected with a *sox10:pax7a* construct at the one-cell stage and reared in embryo medium with methylene blue until 5 dpf ($n = 8$). Boxes indicate area of magnification on the right. Arrowheads indicate a subset of methylene blue–colored xanthophores. Scale bar, 200 µm.

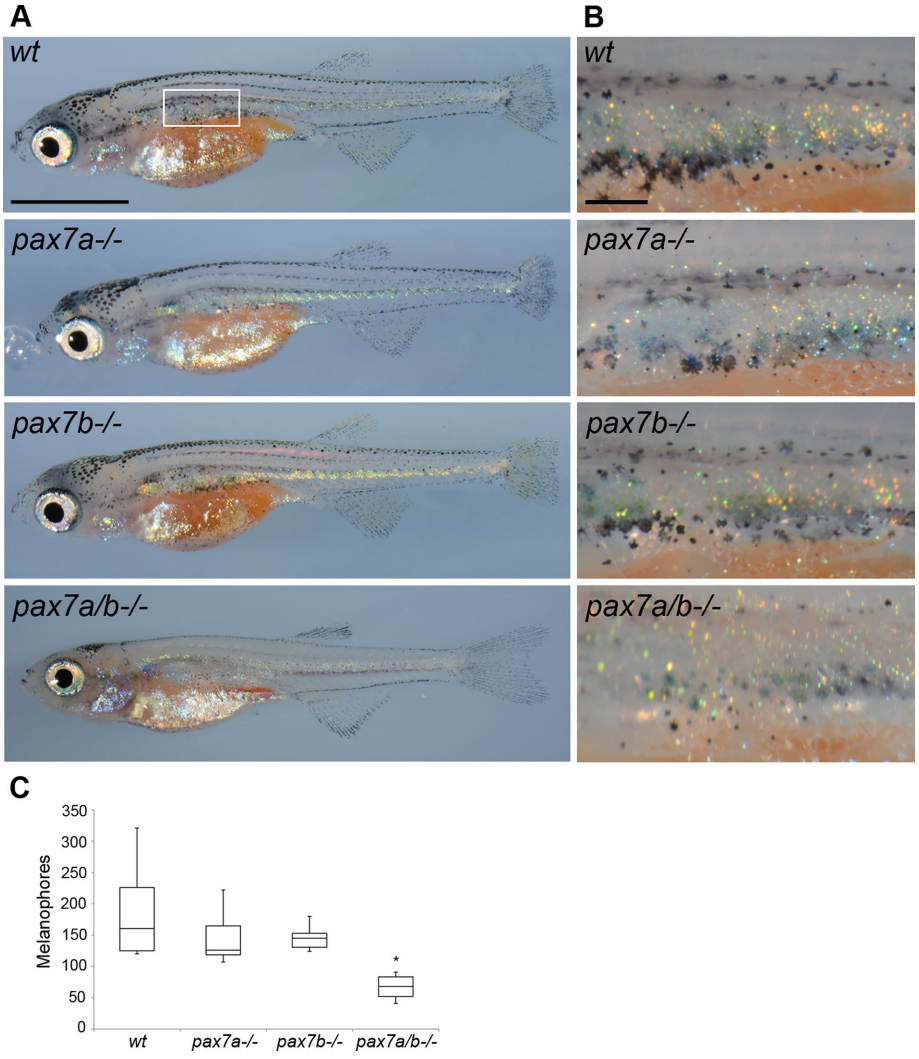

FIGURE 6: The number of melanophores is decreased in *pax7a/pax7b* double-mutant fish during metamorphosis. (A) Pigment phenotype of wt, *pax7a*$^{-/-}$, *pax7b*$^{-/-}$, and *pax7a/pax7b* double-mutant juvenile zebrafish at 30 dpf. Box indicates area of melanophore quantification presented in C. (B) Enlargement of area counted in C. (C) Number of melanophores in wt ($n = 6$), *pax7a*$^{-/-}$ ($n = 8$), *pax7b*$^{-/-}$ ($n = 6$), and *pax7a/pax7b* double-mutant ($n = 10$) juvenile zebrafish at 30 dpf. The *pax7a/pax7b* double-mutant zebrafish differs from all other groups with $p < 0.001$. Comparisons between groups by one-way ANOVA or Kruskal–Wallis ANOVA on ranks with Student's–Newman–Keuls or Dunn's post hoc contrast test for parametric and nonparametric data. Scale bar, 2 mm (A), 200 µm (B).

lack of xanthophores and not only a xanthophore pigmentation deficiency.

To conclude, we present a model (Figure 8) in which either functional Pax7a or Pax7b is required for the establishment of xanthophores in zebrafish. Furthermore, our data show that in the absence of Pax7, there is an expansion of the embryonic and larval melanophore lineage, suggesting that Pax7 is involved in regulating the chromatophore specification process, possibly via a common xanthophore/melanophore precursor cell. In addition, the absence of Pax7 and subsequent lack of xanthophores result in a dramatic melanophore phenotype in juvenile and adult *pax7a/pax7b* double-mutant zebrafish.

MATERIALS AND METHODS

Zebrafish strains and maintenance

Embryos, larvae, and adult fish were maintained from wt zebrafish (*D. rerio*). Mutant lines used were *pax7a*^{umu3} and *pax7b*^{umu4}. Zebrafish were maintained by standard procedures at the Umeå University Zebrafish Facility. All animal experiments were approved by the Umeå djurförsöksetiska nämnd, Dnr: A13-15.

Generation of *pax7a* and *pax7b* mutants using TALENs

TALENs were created using the TAL Effector Kit 2.0 (Cermak *et al.*, 2011) and the RCIscript-GoldyTALEN destination vector (Bedell *et al.*, 2012), both available from Addgene (Cambridge, MA; 1000000024 and 38142). TAL Effector-Nucleotide Targeter (TALE-NT) 2.0 (Doyle *et al.*, 2012) was used for designing the TALENs, with NN repeat-variable diresidues to target guanines. The TALEN pair targeting *pax7a* binds to the sequences 5′-GGAATGG-CTACTTTACCAGGAACAG-3′ (left) and

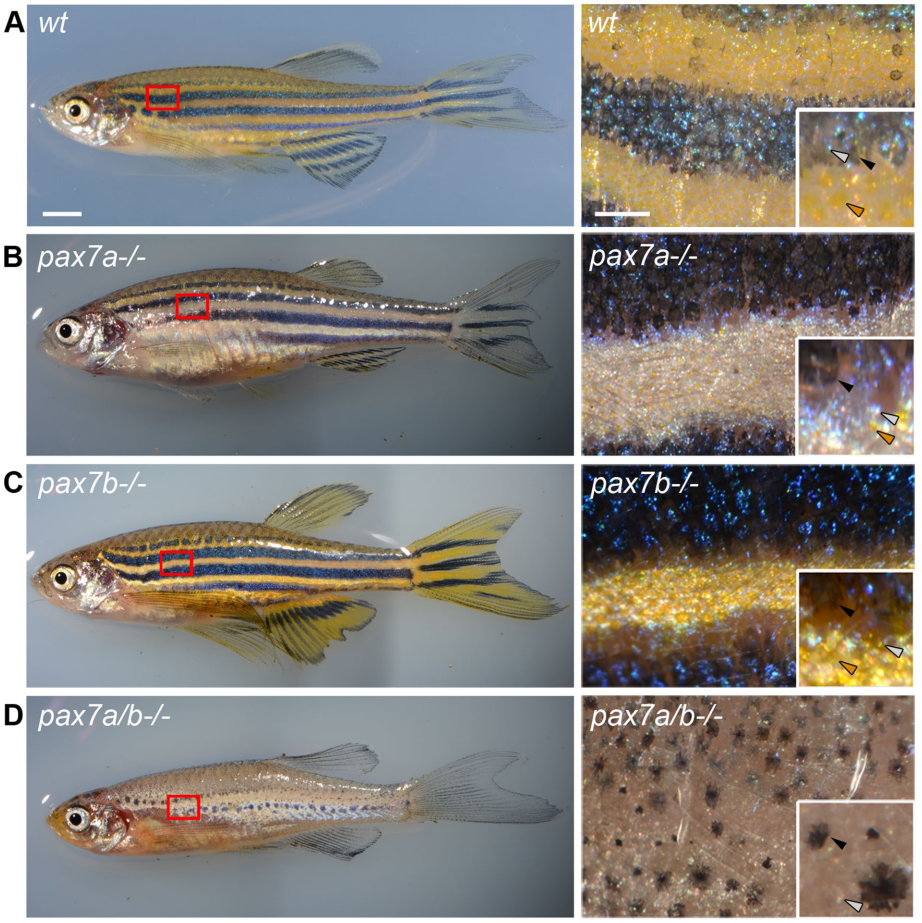

FIGURE 7: The *pax7a/pax7b* double-mutant adult zebrafish has few and disorganized melanophores. Pigment phenotype of 3-mo-old adult (A), wt (B), *pax7a*$^{-/-}$, (C) *pax7b*$^{-/-}$, and (D) *pax7a/pax7b* double-mutant zebrafish. Box indicates area of enlargement on the right. Insets show enlargements visualizing the presence of different types of chromatophores. Black arrowheads indicate melanophores, gray arrowheads indicate iridophores, and orange arrowheads indicate xanthophores. Scale bar, 2 mm (left), 50 µm (right).

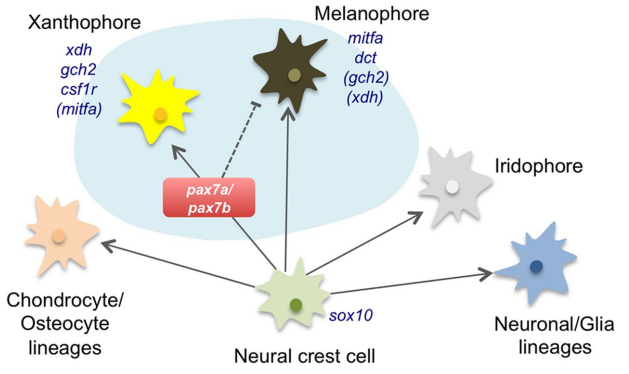

FIGURE 8: Xanthophore specification in zebrafish embryos requires Pax7. The neural crest gives rise to cells of the chondrocyte/osteocyte, neuronal/glia, and chromatophore lineages. Functional Pax7a or Pax7b is required for the formation of xanthophores, and in the absence of Pax7a and Pax7b, the melanophore lineage is expanded, possibly at the expense of xanthophore formation. Markers specific for different chromatoblasts and chromatophores used in this study are depicted.

5′-GGGTAGTTCCTGGCCTGGTGCTG-GCC-3′ (right), and the TALEN pair targeting *pax7b* binds to the sequences 5′-AGAATGTCATCCTTACCGGGAAC-3′ (left) and 5′-AGTTCTGTCCTGGAGCCG-GTCGCA-3′ (right). From 100 to 200 pg of in vitro–generated mRNA (using the T3 mMessage mMachine Kit; Ambion, Austin, TX) of the respective TALEN pair was injected into one-cell-stage embryos. F_0 fish with mutated loci were identified using enzyme restriction digestion of a specific enzyme cut site incorporated in the TALEN spacer sequence of each TALEN pair. We used *Taq*I for identification of *pax7a* mutant embryos and *Bst*UI for *pax7b* mutant embryos before verification by sequencing.

Immunofluorescence

Zebrafish embryos were fixed in 4% paraformaldehyde (PFA) overnight and then stored in 100% methanol at –20°C. Embryos were stepwise rehydrated in PBT (phosphate-buffered saline [PBS] + 0.1% Tween 20) and then acetone cracked for 7 min at –20°C, followed by extensive PBT washing before incubation in blocking solution (PBT + 1% blocking reagent) at room temperature for 1 h. After blocking, embryos were incubated in primary antibody diluted in blocking solution with overnight rocking at 4°C. Embryos were washed 4 × 30 min in PBDTT (PBS, 1% dimethyl sulfoxide, 0.1% Tween 20, 0.5% Triton X-100) and incubated in secondary antibody diluted in blocking solution with overnight rocking at 4°C. Embryos were washed 4 × 30 min in PBDTT and then analyzed. Primary antibodies used were anti-Pax7 (1:10; DSHB, Iowa City, IA; Kawakami *et al.*, 1997), HuC/D (1:200; 16A11; Thermo Fisher Scientific, Waltham, MA), and the secondary antibody used was goat anti-mouse Alexa Fluor 594 (1:500; Molecular Probes, Eugene, OR). 4′,6-Diamidino-2-phenylindole (DAPI) was used to visualize nuclei.

Whole-mount in situ hybridization

Zebrafish embryos were fixed in 4% PFA overnight. Whole-mount in situ hybridization was performed as described previously (Thisse *et al.*, 1993) with minor changes; 1% blocking reagent (Roche, Basel, Switzerland) was used instead of 2% sheep serum and 2 mg/ml bovine serum albumin. Digoxigenin-labeled and fluorescein-labeled RNA probes were detected using 5-bromo-4-chloro-3′-indolyphosphate/nitro blue tetrazolium (Roche) and fast red (Roche). RNA probes were *dct* (Gene Bank accession number BC129260), *gch2* (Gene Bank accession number BC071298), *mitfa* (Gene Bank accession number BC056318), *sox10* (Dutton *et al.*, 2001), and *xdh* and *csf1r* (Parichy *et al.*, 2000). Embryos were analyzed blindly and genotyped postanalysis.

Craniofacial stainings

To detect cartilage, Alcian blue staining was performed. Zebrafish embryos were fixed in 4% PFA overnight and then stored in 100%

methanol at –20°C. Embryos were dehydrated and washed in PBT before being bleached for 2 h in 30% H_2O_2. After further PBT washes, embryos were transferred to Alcian blue solution (1% concentrated hydrochloric acid, 70% ethanol, 0.1% Alcian blue) and incubated overnight. Embryos were washed in acidic alcohol (5% concentrated hydrochloric acid, 70% ethanol), stepwise rehydrated to H_2O, and successively cleared in 20% glycerol with 0.25% KOH and 50% glycerol with 0.25% KOH before imaging. To visualize calcified bone structures, zebrafish were stained with calcein as described previously (Du *et al.*, 2001).

Constructs and microinjections

pax7a RNA (Gene Bank accession number BC163523.1) was generated using the mMESSAGE mMACHINE Kit (Ambion). RNA was microinjected into one-cell-stage embryos at a concentration of 400 ng/µl. The *sox10*:*pax7a* promoter construct was generated using 4118 base pairs of the region upstream of the translational start of *sox10* (National Center for Biotechnology Information reference sequence NC_007114.6) and cloning it in-frame with the translational start of *pax7a* (Gene Bank accession number BC163523.1) or gfp as a control. The construct was injected into one-cell-stage embryos at a concentration of 50 ng/µl.

Cell counts and statistics

To calculate the number of *mitfa*$^+$ and *dct*$^+$ cells, we photographed embryos after in situ hybridization and counted positive cells in the region anterior to the first somite on one side of the embryo; positive cells in the eye were excluded. The average number of positive cells is presented, and Student's *t* test was used to calculate significance. Error bars indicate SEM. For melanophore counts on the crown of the head of 3-dpf embryos and 6-dpf larvae, melanophores on a specific region from the midbrain–hindbrain region to the most anterior part of the dorsal larval melanophore stripe were counted. For more posterior melanophore counts on the dorsal larval melanophore stripe, the dorsal stripe melanophores on somites 8–12 were counted. For melanophore counts during juvenile stages, melanophores in a defined area on the flank of the fish, just above the pectoral fin, were counted. Statistical analyses were performed on SigmaStat, version 3.5 (Systat Software, San Jose, CA). Comparisons between four groups of zebrafish genotypes were analyzed by one-way analysis of variance (ANOVA) or Kruskal–Wallis ANOVA on ranks. Whenever significant, post hoc contrast analyses were performed by Student's–Newman–Keuls test or Dunn's test for parametric and nonparametric data. $p < 0.05$ was considered significant.

Image acquisition and processing

For live imaging, zebrafish were sedated using tricaine mesylate and then placed on a 2% agarose plate and imaged using a Nikon (Tokyo, Japan) SMZ1500 stereomicroscope and a Nikon D5200 digital camera. The same imaging setup was used when imaging embryos stained using in situ hybridization; however, embryos were imaged in 80% glycerol. Immunofluorescently stained embryos were mounted in 80% glycerol and scanned using a Nikon A1 confocal microscope. To visualize early xanthoblasts, live embryos were sedated in embryo medium with tricaine mesylate (ethyl 3-aminobenzoate methanesulfonic acid) and subjected to ultraviolet light as previously described (Le Guyader and Jesuthasan, 2002). Fiji was used for *z*-stack processing and image stitching, and Adobe Photoshop CS4 was used in some instances to enhance contrast and adjust color balance. Comparable sets of images were processed identically.

ACKNOWLEDGMENTS

We thank Christoffer Nord for help with imaging and Eivind Grong for help with statistical analyses. We thank Simon Hughes for the *sox10*, *xdh*, and *csf1r* probes. This work was supported by the Swedish Cancer Society (Cancerfonden), Cancerforskningsfonden Norrland, Magnus Bergvalls Stiftelse, Lennanders Stiftelse, and the Royal Swedish Academy of Sciences.

REFERENCES

Auerbach R (1954). Analysis of the developmental effects of a lethal mutation in the house mouse. J Exp Zool 127, 305–329.

Bagnara JT, Matsumoto J, Ferris W, Frost SK, Turner WA Jr, Tchen TT, Taylor JD (1979). Common origin of pigment cells. Science 203, 410–415.

Basch ML, Bronner-Fraser M, Garcia-Castro MI (2006). Specification of the neural crest occurs during gastrulation and requires Pax7. Nature 441, 218–222.

Bedell VM, Wang Y, Campbell JM, Poshusta TL, Starker CG, Krug RG 2nd, Tan W, Penheiter SG, Ma AC, Leung AY, *et al.* (2012). In vivo genome editing using a high-efficiency TALEN system. Nature 491, 114–118.

Budi EH, Patterson LB, Parichy DM (2011). Post-embryonic nerve-associated precursors to adult pigment cells: genetic requirements and dynamics of morphogenesis and differentiation. PLoS Genet 7, e1002044.

Cermak T, Doyle EL, Christian M, Wang L, Zhang Y, Schmidt C, Baller JA, Somia NV, Bogdanove AJ, Voytas DF (2011). Efficient design and assembly of custom TALEN and other TAL effector-based constructs for DNA targeting. Nucleic Acids Res 39, e82.

Curran K, Lister JA, Kunkel GR, Prendergast A, Parichy DM, Raible DW (2010). Interplay between Foxd3 and Mitf regulates cell fate plasticity in the zebrafish neural crest. Dev Biol 344, 107–118.

Dooley CM, Mongera A, Walderich B, Nusslein-Volhard C (2013). On the embryonic origin of adult melanophores: the role of ErbB and Kit signalling in establishing melanophore stem cells in zebrafish. Development 140, 1003–1013.

Doyle EL, Booher NJ, Standage DS, Voytas DF, Brendel VP, Vandyk JK, Bogdanove AJ (2012). TAL Effector-Nucleotide Targeter (TALE-NT) 2.0: tools for TAL effector design and target prediction. Nucleic Acids Res 40, W117–W122.

Du SJ, Frenkel V, Kindschi G, Zohar Y (2001). Visualizing normal and defective bone development in zebrafish embryos using the fluorescent chromophore calcein. Dev Biol 238, 239–246.

Dushane GP (1934). The origin of pigment cells in Amphibia. Science 80, 620–621.

Dutton JR, Antonellis A, Carney TJ, Rodrigues FS, Pavan WJ, Ward A, Kelsh RN (2008). An evolutionarily conserved intronic region controls the spatiotemporal expression of the transcription factor Sox10. BMC Dev Biol 8, 105.

Dutton KA, Pauliny A, Lopes SS, Elworthy S, Carney TJ, Rauch J, Geisler R, Haffter P, Kelsh RN (2001). Zebrafish colourless encodes sox10 and specifies non-ectomesenchymal neural crest fates. Development 128, 4113–4125.

Eom DS, Bain EJ, Patterson LB, Grout ME, Parichy DM (2015). Long-distance communication by specialized cellular projections during pigment pattern development and evolution. Elife 4, e12401.

Epstein DJ, Vogan KJ, Trasler DG, Gros P (1993). A mutation within intron 3 of the Pax-3 gene produces aberrantly spliced mRNA transcripts in the splotch (Sp) mouse mutant. Proc Natl Acad Sci USA 90, 532–536.

Frohnhofer HG, Krauss J, Maischein HM, Nusslein-Volhard C (2013). Iridophores and their interactions with other chromatophores are required for stripe formation in zebrafish. Development 140, 2997–3007.

Le Guyader S, Jesuthasan S (2002). Analysis of xanthophore and pterinosome biogenesis in zebrafish using methylene blue and pteridine autofluorescence. Pigment Cell Res 15, 27–31.

Hirata M, Nakamura K, Kondo S (2005). Pigment cell distributions in different tissues of the zebrafish, with special reference to the striped pigment pattern. Dev Dyn 234, 293–300.

Irion U, Frohnhofer HG, Krauss J, Colak Champollion T, Maischein HM, Geiger-Rudolph S, Weiler C, Nusslein-Volhard C (2014). Gap junctions composed of connexins 41.8 and 39.4 are essential for colour pattern formation in zebrafish. Elife 3, e05125.

Jostes B, Walther C, Gruss P (1990). The murine paired box gene, Pax7, is expressed specifically during the development of the nervous and muscular system. Mech Dev 33, 27–37.

Kawakami A, Kimura-Kawakami M, Nomura T, Fujisawa H (1997). Distributions of PAX6 and PAX7 proteins suggest their involvement in both early and late phases of chick brain development. Mech Dev 66, 119–130.
Kelsh RN, Brand M, Jiang YJ, Heisenberg CP, Lin S, Haffter P, Odenthal J, Mullins MC, van Eeden FJ, Furutani-Seiki M, *et al.* (1996). Zebrafish pigmentation mutations and the processes of neural crest development. Development 123, 369–389.
Kelsh RN, Schmid B, Eisen JS (2000). Genetic analysis of melanophore development in zebrafish embryos. Dev Biol 225, 277–293.
Kimmel CB, Ballard WW, Kimmel SR, Ullmann B, Schilling TF (1995). Stages of embryonic development of the zebrafish. Dev Dyn 203, 253–310.
Kimura T, Nagao Y, Hashimoto H, Yamamoto-Shiraishi Y, Yamamoto S, Yabe T, Takada S, Kinoshita M, Kuroiwa A, Naruse K (2014). Leucophores are similar to xanthophores in their specification and differentiation processes in medaka. Proc Natl Acad Sci USA 111, 7343–7348.
Lacosta AM, Canudas J, Gonzalez C, Muniesa P, Sarasa M, Dominguez L (2007). Pax7 identifies neural crest, chromatophore lineages and pigment stem cells during zebrafish development. Int J Dev Biol 51, 327–331.
Lacosta AM, Muniesa P, Ruberte J, Sarasa M, Dominguez L (2005). Novel expression patterns of Pax3/Pax7 in early trunk neural crest and its melanocyte and non-melanocyte lineages in amniote embryos. Pigment Cell Res 18, 243–251.
Lang D, Brown CB, Milewski R, Jiang YQ, Lu MM, Epstein JA (2003). Distinct enhancers regulate neural expression of Pax7. Genomics 82, 553–560.
Le Douarin NM, Creuzet S, Couly G, Dupin E (2004). Neural crest cell plasticity and its limits. Development 131, 4637–4650.
Lister JA, Robertson CP, Lepage T, Johnson SL, Raible DW (1999). nacre encodes a zebrafish microphthalmia-related protein that regulates neural-crest-derived pigment cell fate. Development 126, 3757–3767.
Maderspacher F, Nusslein-Volhard C (2003). Formation of the adult pigment pattern in zebrafish requires leopard and obelix dependent cell interactions. Development 130, 3447–3457.
Mahalwar P, Walderich B, Singh AP, Nusslein-Volhard C (2014). Local reorganization of xanthophores fine-tunes and colors the striped pattern of zebrafish. Science 345, 1362–1364.
Mansouri A, Stoykova A, Torres M, Gruss P (1996). Dysgenesis of cephalic neural crest derivatives in Pax7-/- mutant mice. Development 122, 831–838.
Mayor R, Theveneau E (2013). The neural crest. Development 140, 2247–2251.
McMenamin SK, Bain EJ, McCann AE, Patterson LB, Eom DS, Waller ZP, Hamill JC, Kuhlman JA, Eisen JS, Parichy DM (2014). Thyroid hormone-dependent adult pigment cell lineage and pattern in zebrafish. Science 345, 1358–1361.
Minchin JE, Hughes SM (2008). Sequential actions of Pax3 and Pax7 drive xanthophore development in zebrafish neural crest. Dev Biol 317, 508–522.
Monsoro-Burq AH (2015). PAX transcription factors in neural crest development. Semin Cell Dev Biol 44, 87–96.
Murdoch B, DelConte C, Garcia-Castro MI (2012). Pax7 lineage contributions to the mammalian neural crest. PLoS One 7, e41089.
Nagao Y, Suzuki T, Shimizu A, Kimura T, Seki R, Adachi T, Inoue C, Omae Y, Kamei Y, Hara I, *et al.* (2014). Sox5 functions as a fate switch in medaka pigment cell development. PLoS Genet 10, e1004246.
Odenthal J, Rossnagel K, Haffter P, Kelsh RN, Vogelsang E, Brand M, van Eeden FJ, Furutani-Seiki M, Granato M, Hammerschmidt M, *et al.* (1996). Mutations affecting xanthophore pigmentation in the zebrafish, Danio rerio. Development 123, 391–398.
Parichy DM (2006). Evolution of danio pigment pattern development. Heredity 97, 200–210.
Parichy DM, Ransom DG, Paw B, Zon LI, Johnson SL (2000). An orthologue of the kit-related gene fms is required for development of neural crest-derived xanthophores and a subpopulation of adult melanocytes in the zebrafish, Danio rerio. Development 127, 3031–3044.
Parichy DM, Spiewak JE (2015). Origins of adult pigmentation: diversity in pigment stem cell lineages and implications for pattern evolution. Pigment Cell Melanoma Res 28, 31–50.
Parichy DM, Turner JM (2003a). Temporal and cellular requirements for Fms signaling during zebrafish adult pigment pattern development. Development 130, 817–833.
Parichy DM, Turner JM (2003b). Zebrafish puma mutant decouples pigment pattern and somatic metamorphosis. Dev Biol 256, 242–257.
Pelletier I, Bally-Cuif L, Ziegler I (2001). Cloning and developmental expression of zebrafish GTP cyclohydrolase I. Mech Dev 109, 99–103.
Quigley IK, Parichy DM (2002). Pigment pattern formation in zebrafish: a model for developmental genetics and the evolution of form. Microsc Res Tech 58, 442–455.
Raible DW, Eisen JS (1994). Restriction of neural crest cell fate in the trunk of the embryonic zebrafish. Development 120, 495–503.
Simoes-Costa M, Bronner ME (2015). Establishing neural crest identity: a gene regulatory recipe. Development 142, 242–257.
Singh AP, Nusslein-Volhard C (2015). Zebrafish stripes as a model for vertebrate colour pattern formation. Curr Biol 25, R81–R92.
Singh AP, Schach U, Nusslein-Volhard C (2014). Proliferation, dispersal and patterned aggregation of iridophores in the skin prefigure striped colouration of zebrafish. Nat Cell Biol 16, 607–614.
Thisse C, Thisse B, Schilling TF, Postlethwait JH (1993). Structure of the zebrafish snail1 gene and its expression in wild-type, spadetail and no tail mutant embryos. Development 119, 1203–1215.
Tremblay P, Gruss P (1994). Pax: genes for mice and men. Pharmacol Ther 61, 205–226.
Tu S, Johnson SL (2010). Clonal analyses reveal roles of organ founding stem cells, melanocyte stem cells and melanoblasts in establishment, growth and regeneration of the adult zebrafish fin. Development 137, 3931–3939.
Tu S, Johnson SL (2011). Fate restriction in the growing and regenerating zebrafish fin. Dev Cell 20, 725–732.